◆ Human Brain Mapping 34:1357–1370 (2013) ◆

Timing of Posterior Parahippocampal Gyrus Activity Reveals Multiple Scene Processing Stages

Julien Bastin,[1,2,3]* Giorgia Committeri,[4] Philippe Kahane,[2,3] Gaspare Galati,[5] Lorella Minotti,[2,3] Jean-Philippe Lachaux,[6] and Alain Berthoz[1]

[1]*UMR 7152, CNRS-Collège de France, Laboratoire de Physiologie de la Perception et de l'Action, Paris, France*
[2]*Université Joseph Fourier, Fonctions Cérébrales et Neuromodulation, Grenoble, France*
[3]*INSERM U836, Grenoble Institute of Neurosciences, Grenoble, France*
[4]*Department of Clinical Sciences and Bioimaging, University G. D'Annunzio and ITAB, Foundation G. D'Annunzio, Chieti, Italy*
[5]*Department of Psychology, Sapienza University and Laboratory of Neuropsychology, Foundation Santa Lucia, Rome, Italy*
[6]*INSERM U821, Bron, France*

Abstract: Posterior parahippocampal gyrus (PPHG) is strongly involved during scene recognition and spatial cognition. How PPHG electrophysiological activity could underlie these functions, and whether they share similar timing mechanisms is unknown. We addressed this question in two intracerebral experiments which revealed that PPHG neural activity dissociated an early stimulus-driven effect (>200 and <500 ms) and a late task-related effect (>600 and <800 ms). Strongest PPHG gamma band (50–150 Hz) activities were found early when subjects passively viewed scenes (scene selectivity effect) and lately when they had to estimate the position of an object relative to the environment (allocentric effect). Based on single trial analyses, we were able to predict when patients viewed scenes (compared to other visual categories) and when they performed allocentric judgments (compared to other spatial judgments). The anatomical location corresponding to the strongest effects was in the depth of the collateral sulcus. Our findings directly affect current theories of visual scene processing and spatial orientation by providing new timing constraints and by demonstrating the existence of separable information processing stages in the functionally defined parahippocampal place area. *Hum Brain Mapp 34:1357–1370, 2013.* © 2012 Wiley Periodicals, Inc.

Key words: retrosplenial; collateral sulcus; egocentric; gamma oscillations; allocentric; spatial cognition; visual recognition; direct human recordings; EEG; frames of reference

Additional Supporting Information may be found in the online version of this article.

Contract grant sponsor: NeuroProbes (EU Research Program; J.B.); Contract grant number: FP6-IST 027017.

*Correspondence to: Julien Bastin, Inserm U.836, Institut des Neurosciences de Grenoble, Bâtiment Edmond J. Safra des Neurosciences, Chemin Fotuné Ferrini, Université Joseph Fourier, Site Santé La Tronche, BP 170 38042 Grenoble Cedex 9, France. E-mail: julien.bastin@ujf-grenoble.fr

Received for publication 18 July 2011; Revised 11 October 2011; Accepted 17 October 2011

DOI: 10.1002/hbm.21515
Published online 30 January 2012 in Wiley Online Library (wileyonlinelibrary.com).

INTRODUCTION

Locating ourselves and objects within the environment requires the parallel operation of egocentric (i.e., relative to the body) and allocentric (i.e., relative to external reference points) spatial information processing [Burgess, 2006]. One can also shift rapidly from one reference frame to the other. For instance, when using a global positioning system (GPS), we need to shift from the allocentric map indications of the GPS to the egocentric view of the environment. Although we routinely perform such operations to orient ourselves and to navigate, the brain dynamics underlying egocentric and allocentric visual scene encoding remain poorly understood. Lesion studies have shown the critical involvement of the hippocampus, the posterior parahippocampal gyrus (PPHG) and the retrosplenial cortex (RSC) in topographical tasks [Bohbot et al., 1998; Maguire, 2001]. In the latest years, particular interest has been devoted to a subregion of the PPHG, called parahippocampal place area (PPA) because of its selective and automatic response to passively viewed scenes [Epstein and Kanwisher, 1998]. Neuroimaging studies showed that besides encoding the spatial layout of scenes [Epstein and Kanwisher, 1998; Park et al., 2007], this area is involved in objects/landmarks localization [Aguirre et al., 1998; Committeri et al., 2004; Janzen and van Turennout, 2004; Maguire et al., 1998] and contextual processing [Bar, 2004; Epstein and Ward, 2009].

A large body of electrophysiological evidences related to spatial representation comes from rodent studies. The parahippocampal region in the rodent brain includes entorhinal cortex, presubiculum, and parasubiculum [Furtak et al., 2007; Sugar et al., 2011]. In presubiculum [Taube et al., 1990] and in other brain areas of the Papez circuit [Taube, 2007], head direction (HD) cells fire as a function of the rats' head orientation relative to the environment (independently from its location). In presubiculum and parasubiculum, border cells encode distance to environment borders [Boccara et al., 2010] and grid cells encode multiple environment locations corresponding to a geometrical grid array [Boccara et al., 2010; Moser et al., 2008]. In the hippocampus, place cells encode the animal location within the environment independently from its orientation [Burgess and O'Keefe, 2011; O'Keefe, 1976] and "boundary vector cells" encode both distance and direction to environment borders [Lever et al., 2009]. In the RSC, HD cells were also identified [Chen et al., 1994]. Despite the large number of studies performed in rodents, the functional role of these regions in humans was not yet fully characterized, especially because combinations of electrophysiological recordings and spatial tasks in humans are rare [but see Caplan et al., 2003; Ekstrom et al., 2003; Jacobs et al., 2010].

Given its deep anatomical location, the role of PPHG electrophysiological activity (i.e., its activity observed at the trial level/at the millisecond time scale) is best characterized using invasive electrophysiological methods. Rare intracerebral recordings performed during spatial tasks or visual recognition tasks revealed neural activity in the hippocampus, parahippocampal gyrus and the bordering collateral sulcus (COS) with latencies within PPHG ranging from 200 to 500 ms after stimulus presentation [Kraskov et al., 2007; Liu et al., 2009]. However, these studies did not report scene selective oscillatory modulations within the PPHG and neurons were surprisingly found to be less selective compared to other medial temporal lobe regions [Mormann et al., 2008]. To date, only one study [Kraskov et al., 2007] examined PPHG scene selectivity and reported no scene specific oscillatory modulations although firing rate in parahippocampal gyrus (PHG) was modulated by stimulus category in some of the recorded PHG sites (though in only five of 47 recorded sites).

Here, we recorded directly PPHG and adjoining COS activity using deep brain electrodes implanted for clinical purposes in epileptic patients to dissociate egocentric from allocentric frame of reference use. In a first experiment, we asked patients to perform a relative distance judgment task successfully used previously in fMRI [Committeri et al., 2004]. An example of the problem subjects had to face in this paradigm is if we ask the reader of this article: "Is your computer screen parallel to your office's building entrance?" Trying to respond to such question requires the reader to shift from a viewer-centered to an environment-centered reference frame, assuming the building entrance is not directly visible and therefore needs to be retrieved from a mental map of the building stored in memory. We used sets of scenes depicting a three-winged palace (Fig. 1) and two target objects (dustbins) placed on the ground. Subjects were asked to perform two types of judgments: (i) which of the two targets was closer to their bodies (egocentric condition, Ego) and (ii) which of the two target objects was closer to the central wing of the palace (Allocentric condition, Allo). Importantly, to induce a mental reconstruction of the environment to solve the Allo task, the scenes comprised only a partial view of the spatial layout (Fig. 1) so that it was necessary to reconstruct mentally the environmental geometry to recognize the central wing as a function of the lateral wings of the palace in the allocentric condition, a process that will be referred later on to allocentric processing. Experiment 2 (PPA localizer) was designed to functionally define PPA (scenes $>$ objects), thus enabling a comparison between scene recognition and spatial processing time within PPA. Our results show that neurophysiological activity in PPHG dissociates an early scene categorization response (i.e., stimulus specific) from a late task-specific response (i.e., allocentric processing) in the gamma band (50–150 Hz). Additionally, single trials analyses were successfully used to predict whether the patient was looking at a scene or not and whether the patient was asked to make allocentric or egocentric judgments.

MATERIAL AND METHODS

Subjects

Eight patients suffering from drug-resistant partial epilepsy (P1–P8) were included in this study. They were all

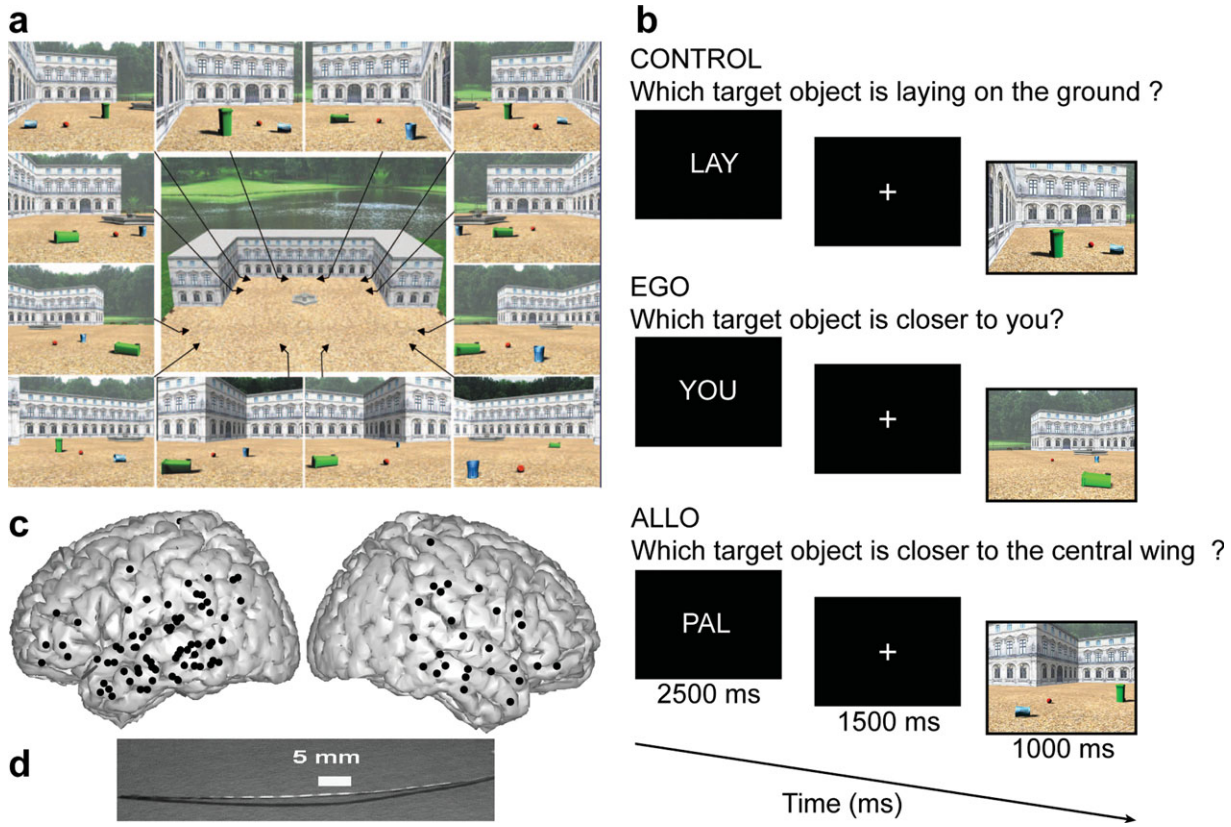

Figure 1.

Experimental design used to dissociate reference frame for spatial cognition (**a** and **b**) and entry points and structure of implanted intracerebral electrodes (**c** and **d**). (a) Viewpoints used to generate scenes stimuli. Objects positions within the scenes were independently manipulated relative to viewpoints. (b) Stimulus sequence. The main task was to judge which of the two target objects was closer to the patient's body/viewpoint (EGO) or which target object was closer to the central wing of the palace (ALLO). The control condition (CON) did not require position or distance estimation but required a shift of attention within the scene. The lower timeline shows the duration of each stimulus. (c) Electrodes entry point represented on a 3D reconstruction of the MNI brain. Each dot corresponds to a 1D array penetrating the brain orthogonally to the sagittal plane. (d) Multisites depth electrode. PAL, Palace (task instruction given before allocentric trials); YOU (task instruction given before egocentric trials); LAY, Laying (instruction given before control trials). [Color figure can be viewed in the online issue, which is available at wileyonlinelibrary.com.]

right-handed females and had normal vision without corrective glasses. Patient age was 29.4 ± 10.1 (mean ± standard deviation). Because the location of the epileptic focus could not be identified using noninvasive methods, the patients underwent intracerebral recordings by means of stereotactically implanted multilead depth electrodes (sEEG).Selection of sites to implant was adapted to the suspected origin of seizures, therefore with no reference to the present experimental protocol. However, these patients were included into this experiment because their implantations sampled several areas located in the medial occipitotemporal cortex. Patients had previously given an informed consent to participate in the experiment which was approved by the Grenoble medical ethical committee.

Electrode Implantation and Recordings

Twelve to 16 semirigid electrodes were implanted depending on the patient; each electrode had a diameter of 0.8 mm and comprised 6–18 leads of 2 mm, 1.5 mm apart (Dixi, Besançon, France), depending on the target region. The electrode contacts were identified on each individual stereotactic scheme and then anatomically localized using the proportional atlas of Talairach and Tournoux after a linear-scale adjustment used to correct for size differences between the patient's brain and the brain in the Talairach's atlas. In addition, these anatomical location were determined via a second computer-assisted procedure, consisting of directly visualizing the electrode positions on the patient's MRI (i.e., by matching the

postimplantation CT-scan showing the contact sites with the preimplantation three-dimensional (3D) MRI, using VOXIM R, IVS Solutions, Germany). Note that multilead depth electrodes were usually implanted orthogonal to the interhemispheric plane, and by convention lower electrode contacts' labels are more medial. Recordings were conducted using an audio–video-EEG monitoring system (Micromed, Treviso, Italy), which allowed the simultaneous recording of 128 depth-EEG channels sampled at 512 Hz [0.1–200 Hz bandwidth]. One of the contact sites in the white matter was chosen as reference. Figure 1 shows the anatomical location of the entry points of the electrodes implanted for the eight patients. Electrode contacts were located in the medial temporal cortex, at the level of the middle-posterior COS, thus covering part of the parahippocampal gyrus (PHG), and more ventrally the fusiform gyrus (FUG). Additionally, some electrode contacts were implanted in the RSC, in the superior and middle temporal gyri, in inferior frontal and parietal cortices (Supporting Information Table S1).

Experiment 1

We used a 3D realistic reconstruction of a complex environment, representing a square arena in front of the entrance of a palace (see [Committeri et al., 2004] for a detailed description on stimuli generation). The arena was defined by the two short lateral wings and the long central wing of the palace (Fig. 1). During the experiment, the patients were shown a different snapshot (of about 18 × 14° of visual angle) of the environment in each trial. Each snapshot simulated a photograph of the environment taken from one of 12 different points of view. The only constraint was that at least part of the long central wing of the palace was always visible. The small panels in Figure 1 show the chosen camera positions and the corresponding snapshots. In each snapshot, three different objects were also visible: two target objects (a big green and a small blue garbage can) and one reference object (a red ball). These three objects occupied a different position in each trial. Moreover, one of the two garbage cans was lying on the ground in each snapshot (see [Committeri et al., 2004] for more details on the environment and the stimuli construction).

The patients were asked to judge which of the two target objects was closer to the central wing of the palace (environment-centered allocentric condition, Allo), or closer to their point of view (egocentric condition, Ego). While the Ego condition required the use of an egocentric frame of reference to complete the distance judgment, the Allo condition required to use environmental knowledge to solve the task. More specifically, in the Allo condition, patients had to access a mental reconstruction of the environment to recognize the central wing as a function of the lateral wings.

To manipulate independently egocentric and allocentric scene processing, target locations were changed both with respect to the environmental landmark and with respect to the point of view used to generate the scene in each trial. Hence, egocentric (allocentric) object location was made irrelevant in the allocentric (egocentric) condition. A control task was added to account for low-level visual and motor response processes that were not related to distance estimation and reference frame use. In this control task (Con), patients had to judge which of the two target objects was lying on the ground, thus focusing on object orientation. Before the experimental session, the patients underwent a short preliminary training session (<5 min). First, they were shown a 1-min animation on a computer screen simulating a rapid circular walking in the environment, to familiarize with it. Then patients were instructed about tasks, and started to perform training trials in which a reduced set of the experimental stimuli was used, to allow a first approach to the response procedure.

The experiment consisted in eight sessions of 5 min composed of 12 randomized blocks of six successive trials lasting 18 s each. The first patient (P1) was unable to conclude the last session, responding to 72 blocks. At the beginning of each block, an instruction about the task and condition to perform during the incoming block appeared in the middle of the screen for 1.5 s, followed by a 0.4° fixation cross for 1.5 s. A series of six 2.5-s trials followed. In each trial, a snapshot of the environment appeared for 1 s, followed by a white fixation cross appearing on a black background for 1.5 s. Such a fast presentation rate was chosen to minimize eye movements, which were shown to be identical in all three spatial conditions [Committeri et al., 2004].

Experiment 2

Series of five pictures corresponding to distinct visual categories (i.e., scenes, houses, objects, faces, tool, animal, scrambled, and fruits) were presented to the patient, each stimulus presentation lasting 200-ms interleaved with a variable interstimulus interval (ISI) during which a white fixation cross was displayed on a black screen (average ISI = 800 ms). Each block of five-picture presentation was followed by a 2,000-ms blinking period followed by a fixed fixation inter stimulus interval (1,500 ms) preceding the next block of five trials. To ensure that patients were performing the effectively task, we asked them to press a response button whenever they saw a "fruit" stimulus.

Apparatus

The visual stimuli were delivered in both experiments on a CRT monitor with a refresh rate of 60 Hz, controlled by a PC (Pentium 133, Dos) with Presentation (Neurobehavioral Systems, Albany, CA). To control the timing of stimulus delivery, a TTL (transistor-transistor logic) pulse was sent by the stimulation PC to the EEG acquisition PC. The patients were seated in a dimly lit, electrically shielded, and sound attenuated room, with response buttons under their right hand.

Data analyses

Electrophysiological analyses were restricted to electrodes located outside epileptic foci and to successful trials. For each single trial, bipolar derivations were computed between adjacent electrode contacts to suppress contributions from nonlocal assemblies and assure that the bipolar SEEG signals could be considered as originating from a cortical volume centered within two contacts (the intracontact distance was 1.5 mm). The spatial resolution of such bipolar recordings has been estimated as being around 4 mm [Lachaux et al., 2003], which is comparable with the standard fMRI voxel size. Bipolar derivations were first analyzed by averaging the signal corresponding to each condition to compare the event-related potentials (ERP) obtained in each experimental condition.

To quantify signal power modulations across time and frequency we used standard time-frequency (TF) wavelet decomposition. The signal $s\ (t)$ is convoluted with a complex Morlet wavelet $w\ (t, f_0)$, which has Gaussian shape in time (σ_t) and frequency (σ_f) around a central frequency f_0 and defined by: $w\ (t, f_0) = A \exp\ (-t^2/2\sigma^2{}_t) \exp\ (2i\ \pi f_0 t)$, with $\sigma_f = 1/2\pi\sigma_t$ and a normalization factor $A = (\sigma_t\sqrt{\pi})^{-1/2}$. Throughout this study, we used a wavelet family with cycle number set to 7 (i.e. $f_0/\sigma_f = 7$). The square norm of the convolution results in a time-varying representation of spectral power, given by: $P\ (t,f_0) = |\ w\ (t, f_0) \times s\ (t)\ |^2$. Significant spectral modulations and evoked responses relative to the fixation period immediately preceding each stimulus presentation were detected using a Wilcoxon nonparametric test that compared, across the trials, the total energy in a given TF tile [100 ms × 1 Hz], with that of a tile of similar frequency extent covering a prestimulus baseline period [from −800 to −500 ms]. The overlap was set at 100% in the frequency domain (i.e., step was set to 1 Hz) and 50% in the time domain (step = 50 ms).

TF regions with significantly energy modulations compared to stimulus preceding baseline level were defined for each electrode bipolar derivation and identified as TF regions of interest (TFROIs). Each TFROI energy was then compared across the different experimental conditions using Kruskal–Wallis nonparametric tests (in the text: KW). KW tests were first applied to the raw TF values of energy, on a set of TF tiles [100 ms × 8 Hz] covering a [−500:2,000 ms × 13:150 Hz] domain with an overlap of 50% in both the time and frequency axis (one test per tile comparing the values obtained for all the trials in the two conditions). To analyze lower frequency oscillations, another mesh was used with time frequency tiles of [100 ms × 2 Hz] covering a [−500:2,000 ms × 2:13 Hz] domain with an overlap of 50% in both the time domain and in the frequency domain. A second procedure was used to illustrate the time course of power in a given frequency band, and to confirm all the results obtained using the wavelet-based approach. Raw signals were band-pass filtered in 10 consecutive frequency bands (from [50–60 Hz] to [140–150 Hz], by steps of 10 Hz), and for each band, the envelope of the band-pass filtered signal was computed with a Hilbert transform. For each band, this envelope signal was divided by its mean value across the entire recording session and multiplied by 100 so that envelope values are expressed in percent of that mean value. Finally, the envelope signals computed for each of the 10 frequency bands were averaged together, to provide one single time-series (the gamma-band envelope) for the entire session. By construction, the mean value of that time-series across the recording session is equal to 100.

We used a baseline [–250 to 0 ms] and a test ([0 to 1000] and [0 to 600 ms], respectively, for Experiments 1 and 2) time intervals to run two separate ROC analyses. The inputs of the ROC were the average gamma-band power in each trial in either the baseline or the test period. The hit rate (y-axis) was defined as the relative number of allocentric (scene/house) trials with a response larger than a sliding threshold. Similarly, the false positive rate (x-axis) was defined as the relative number of control/egocentric (face/objects/other categories except fruits) trials with a response larger than the sliding threshold. ROC curves were obtained by gradually lowering the threshold. Starting with a very high threshold (no hits, no false positives), if there is a larger gamma-band response for allocentric (scene) trials, the ROC curve will show a steep increase when lowering the threshold. If the gamma-band power responds equally to allocentric (scene) and other trials type, it will have a similar relative number of hits and false positives, and the ROC curve will fall along the diagonal. In the first case, the area under the ROC curve will be close to 1, whereas in the latter case it will be ≈0.5. To estimate statistical significance, we compared ROC areas obtained over the baseline period with those obtained in the test period with separate student t-tests for Experiments 1 and 2 ROC analyses.

Behavioral measures (accuracy and reaction times, RT) were submitted to (parametric) a repeated measures analyses of variance when the data conformed to a normal distribution whereas nonparametric tests were applied when appropriate. The statistical threshold corresponding to significance was set at $P = 0.05$. The statistical results reported were corrected for multiple comparisons when appropriate using the false discovery rate (FDR) algorithm [Genovese et al., 2002].

RESULTS

Behavioral Responses

Patients could adequately perform the task, and all three experimental conditions were found equally easy according to the mean accuracy of judgments (92.9, 91.7, and 95.4% in the Allo, Ego, and Con conditions, respectively, Supporting Information Fig. S1). Furthermore, patients spent the same time to solve the task in all conditions. The mean RT of correct responses corresponded to the latency of the stimulus

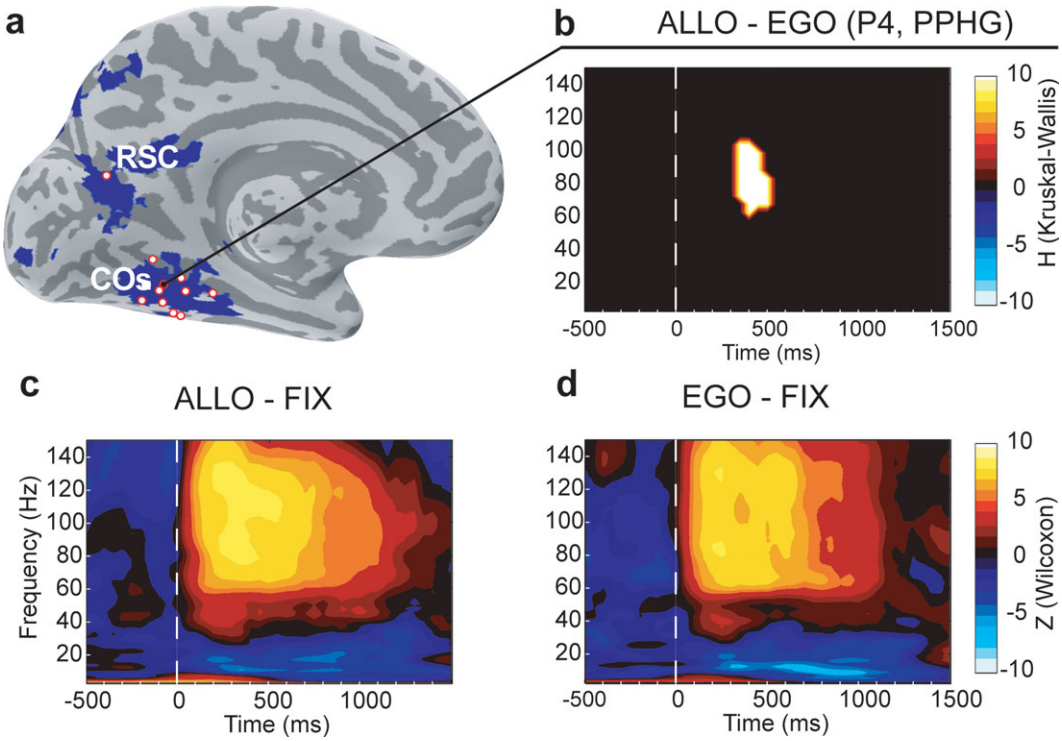

Figure 2.

Typical pattern of oscillatory activity recorded from a PPHG site (patient P4, x′5, **b–d**) and group PPHG sites anatomical location relative to brain areas specialized for allocentric coding as defined from a previous fMRI study (**a**). (a) Bold contrast Allo > Ego from a previous fMRI study (Committeri et al., 2004) is shown in blue on the inflated MNI brain. Electrode contacts from all patients located at the vicinity of the collateral sulcus or retrosplenial cortex are superimposed (red dots). (b) Typical allocentric statistical effect observed in an individual PPHG (Allo > Ego, Patient 4, KW test FDR corrected) was only observed in the gamma band (50–150 Hz). A positive H value (extracted from KW tests) corresponded to regions in the time-frequency space where PPHG activity was stronger in the allocentric condition compared to the egocentric condition. (c and d) Time-frequency representation of the electrophysiological responses recorded in the same PPHG site of Patient 4 (P4) in the Ego (c) and Allo (d) conditions. Warmer (yellow) colors correspond to a significant (Wilcoxon tests) power increase relative to baseline (−800 to 500 ms before stimulus), whereas cooler (blue) colors correspond to power significant power decreases. Wilcoxon tests were not corrected for multiple comparisons with FDR for illustrative purposes. [Color figure can be viewed in the online issue, which is available at wileyonlinelibrary.com.]

disappearance at 1,000 ms (RT was, respectively, 970, 996, and 927 ms in Allo, Ego, and Con conditions, Supporting Information Fig. S1). Statistical analyses revealed that there was no significant effect of spatial condition, neither on RT (Kruskal-Wallis test, KW = 1.396; $P = 0.497$), nor on success rate ($F_{(2,14)} = 2.94$; $P = 0.0856$). Therefore, a global difference of attention and/or task difficulty cannot account for the following electrophysiological results.

Gamma-Band Activity in PPHG Dissociates Spatial Frame of Reference Used During Scene Processing

Posterior parahippocampal sites ($n = 15$, see Supporting Information Table S1 for Talairach's coordinates) were recorded in five patients. To test the effect of using distinct frames of reference to process a visual scene, electrophysiological responses recorded in the egocentric, allocentric, and control conditions were compared. A first statistical analysis was performed on the TF power values recorded across trials (Supporting Information Table S2) for each PPHG electrode contact separately (see Fig. 2b for a representative PPHG site). This analysis did not reveal any significant differences between spatial conditions until the first peak of activity (250 ms after stimulus onset). Furthermore, only gamma-band activity was task specific. Indeed, gamma-band activity increased during stimulus presentation whatever the spatial condition (Fig. 3), but this activity was of higher amplitude and lasted longer for allocentric judgments compared to egocentric and control judgments (in the 200–800 ms range), as confirmed by the statistical analyses performed for each PPHG site (Fig. 3; $P < 0.05$). Furthermore, gamma activity was of higher

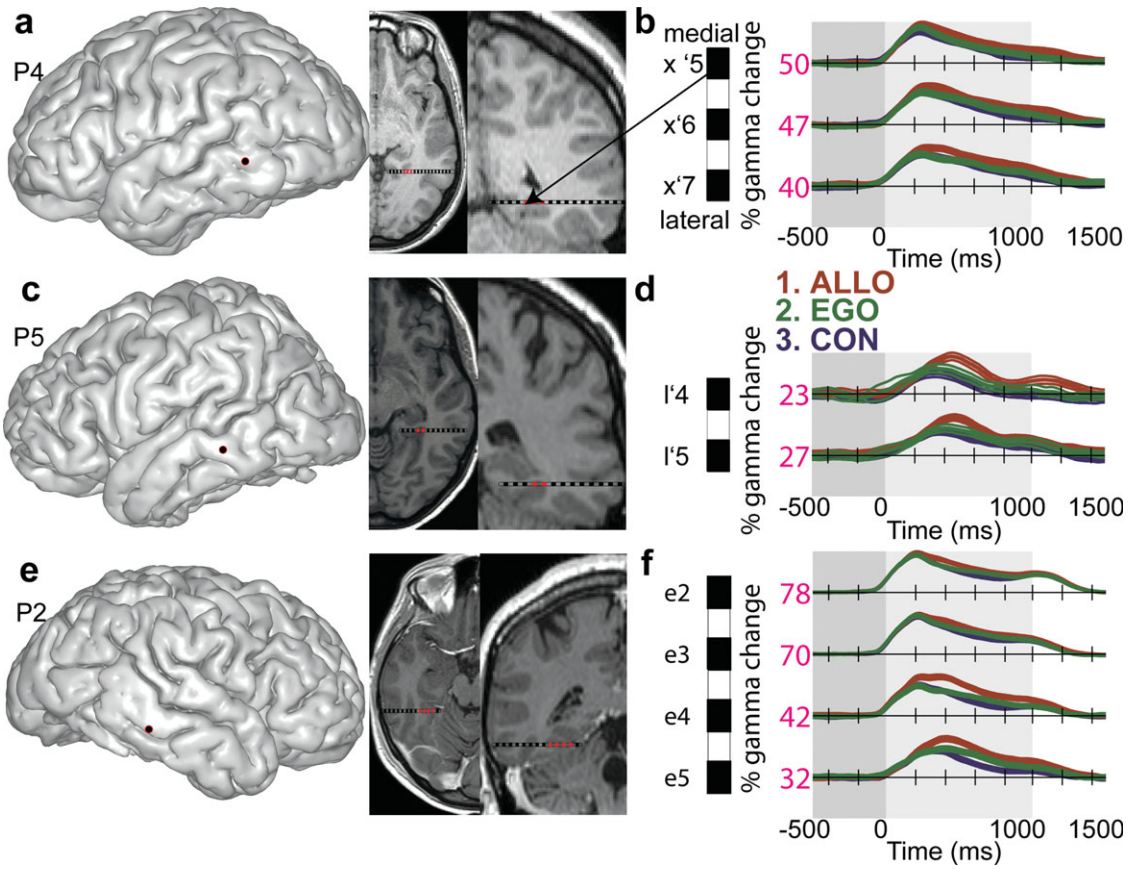

Figure 3.

Reproducibility across patients of gamma-band time courses as a function of spatial conditions in PPHG. (**a**, **c**, and **e**) Individual anatomical location of the electrode entry point on the patient's 3D brain is shown in addition to sagittal and coronal MRI slices (radiological convention) corresponding to the PPHG electrode contacts. (**b**, **d**, and **f**) Mean energy time courses (±95% confidence intervals) in the high gamma frequency band (50–150 Hz) is represented for all three conditions, expressed as a percentage of increase. The maximal value recorded for each electrode contact is also indicated (32). Lower case letters indicate different electrodes in each patient and the assigned numbers refer to the contact site within that electrode, with numbers increasing in the medial-to-lateral direction. Electrodes in the left hemisphere are indicated by (′) between the electrode letter and the contact site number (e.g., x′5–x′7 for patient P4), whereas right hemisphere electrodes are not (e.g., e2–e5 for patient P7). [Color figure can be viewed in the online issue, which is available at wileyonlinelibrary.com.]

amplitude in the PPHG during egocentric judgments compared to the control condition (Fig. 3; $P < 0.05$). The reproducibility across patients and recording sites of the gamma-power time course as a function of experimental condition was very high (Figs. 3 and 6), and the anatomical location of PPHG sites was also very consistent across patients, close to the depth of the COS.

Figure 4 illustrates the group (across patients) time course of PPHG activity ($n = 15$). Figure 4 illustrates the time course of averaged PPHG gamma activity across patients ($n = 15$ PPHG sites). An analysis of group confirmed that gamma-band activity time course dissociates all three spatial tasks (Allo > Ego > Con). PPHG gamma amplitude modulations as a function of was analyzed using a repeated measures ANOVA with factors time (five 200 ms time bins covering stimulus presentation [0:1,000 ms]) and spatial conditions. The analysis revealed a significant time interval × spatial condition interaction ($F_{(8,112)} = 26.50$; $P < 10^{-6}$). To further interpret this interaction, post hoc tests (Scheffé) were performed. We found that gamma-activity amplitude and duration varied depending on the experimental condition (Con, Ego, Allo), In the control condition, there was a significant gamma increase between 200 and 400 ms. In the egocentric condition, gamma increase lasted significantly longer (from 200 to 600 ms, Fig. 4), and gamma amplitude was higher relative to the control condition in the [400 to 600 ms] (Fig. 4). Finally, gamma PPHG activity triggered by the allocentric condition differed from control and egocentric conditions respectively in the 400–800 and 600–800 ms range.

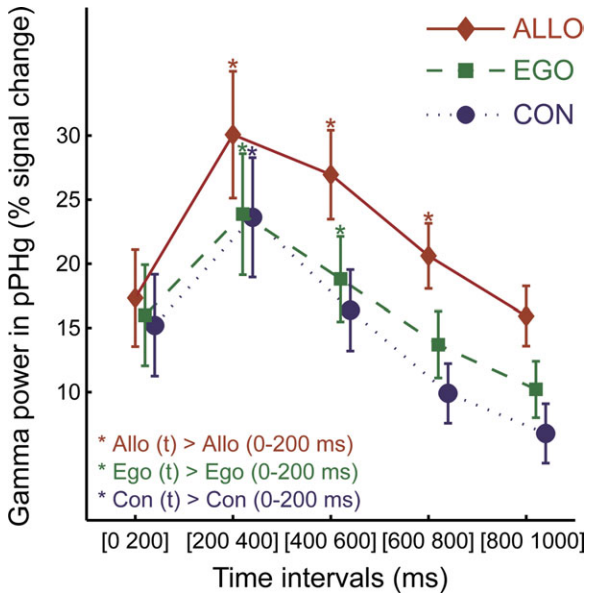

Figure 4.

Time course of the group averaged PPHG gamma activity (mean ± standard error) as a function of spatial conditions ($n = 15$ PPHG sites). Significance markers (*) reflect the results of the posthoc analysis performed to detail the time interval × spatial condition ANOVA interaction. For each spatial condition, the first time interval (0–200 ms) was compared to other time intervals to directly compare the duration of the gamma-band increase in the allocentric, egocentric, and control conditions. The interaction corresponds to the fact that gamma activity was shorter in the control condition (< 400 ms), slightly longer in the egocentric condition (< 600 ms) and longest in the allocentric task (< 800 ms). [Color figure can be viewed in the online issue, which is available at wileyonlinelibrary.com.]

Single Trial Predictions of Allocentric Frame of Reference Use

On the basis of single trial PPHG activity, we then asked if we could predict the type of spatial judgment performed by patients. This type of analyses has been conducted successfully in animal studies to operate single-neuron response readout [Britten et al., 1992] and to interpret response specificity of intracranial ERP [Liu et al., 2009] as well as specificity of noninvasive magnetoencephalography spectral power signals [Vidal et al., 2010] in humans. This type of analysis formally demonstrates the specificity of neural activity, and quantify how sufficient is this specificity to infer what task was performed from single trials. Task differences (Allo, Ego, and Con) were strong enough to be directly visible in single trials data (Fig. 5a). To quantify the degree of discrimination that could be obtained using single trials data, a receiver operator characteristic (ROC) analysis was used [see Quiroga et al., 2008 for a similar procedure], and ROC curves were computed for each PPHG site (Fig. 5b). If the gamma-band response is reliably higher across trials in the allocentric condition relative to the control and egocentric conditions (as demonstrated above), the ROC curves will have an area under curve (AUC) close to 1 whereas if one cannot predict from single trials what spatial condition the patient is performing, ROC curves will have an AUC close to 0.5 (see Material and Methods). AUC values, thus, index the performance of an ideal observer to discriminate spatial judgments performed by patients using the amplitude of gamma activity as a decision threshold.

Allocentric trials could be reliably discriminated from control and egocentric trials (Fig. 5c; $P < 0.05$). Discrimination performance was above chance level: we used a baseline window preceding stimulus onset and compared AUC values obtained during this baseline to AUC values obtained during stimulus presentation (we used an early 500-ms time window or a late 500-ms time window). Egocentric trials were less reliably discriminated from control trials: ROC performance was lower and more variable compared to allocentric trials, although performance was above chance levels ($P < 0.05$, only for the second 500-ms stimulus period). These analyses extend results based on averaged PPHG activity to single trial level.

PPA Dynamics Reveal an Automatic Scene Recognition Process (PPA Localizer)

To examine whether recorded PPHG sites could correspond to the functionally defined PPA region, two patients (P7 and P8, $n = 6$) performed a PPA localizer (Fig. 6). Gamma activity was significantly higher and lasted longer when patients viewed scenes (i.e., gamma increase was observed from 200 to 500 ms) compared to when patients viewed objects (i.e., a scene effect). This effect was significant in five of six PPHG sites (P7 e2–4 and P8 d′2–3, 6e–f; $P < 0.05$) where the allocentric effect was also observed (Fig. 6c,d). In addition to defining functionally PPA with gamma-band activity, Experiment 2 also provide interesting data to compare the latencies of stimulus specific effect (the scene effect) and task specific effect (allocentric effect). Striking timing differences were found in both patients: the earliest effect was the scene effect whereas a longer latency effect corresponded to allocentric processing.

Single Trial Decoding of Visual Scene Encoding

The effect of scene stimuli on gamma-band amplitude was so robust that it could be seen directly in single trials (Fig. 6i,j). To quantify how reliably an ideal observer could decode the stimulus category that was seen by the patient using single trial PPA gamma-band amplitude, we performed again a ROC analysis. Supporting Information Figure S2 shows discrimination values for all PPA sites. We compared a 250-ms baseline period preceding the stimulus with a test period (0–600 ms from stimulus onset). In the baseline period, the median of A' distribution was

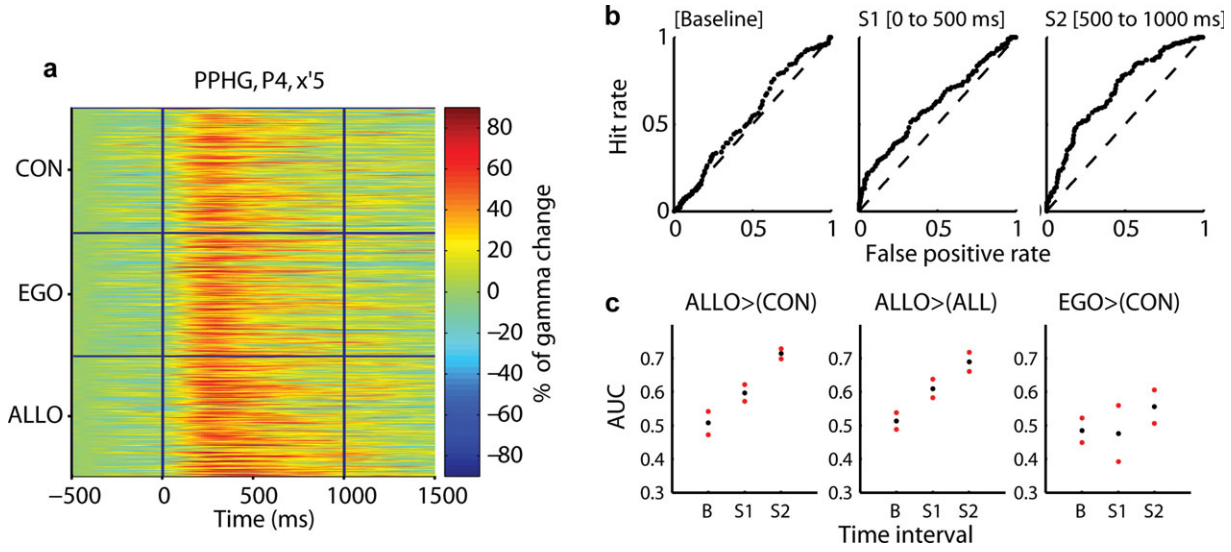

Figure 5.

Selective single trial PPHG gamma amplitude increases in allocentric trials. (**a**) Example of single trial neural gamma-band modulation expressed in percentage of change relative to baseline (P4, x′5). The electrode contact elicited a strong preference to allocentric processing. (**b**) Receiver operator characteristic (ROC) curves obtained by contrasting allocentric trials to all other trial types in three time intervals (same electrode as in a). (**c**) Average area under curves (AUC) extracted from ROC analyses in all PPHG sites ($n = 15$) and 95% confidence intervals. Allocentric trials could be readout when compared to control (left panel), to control and egocentric trials (middle panel), whereas egocentric trials were harder to discriminate although performance was above chance level (right panel). Baseline period, B = (−250 to 0 ms). Stimulus period S_1 = (0–500 ms); stimulus period S_2 = (500–1,000 ms poststimulus onset). [Color figure can be viewed in the online issue, which is available at wileyonlinelibrary.com.]

significantly lower (0.47) compared to A' median in the test period ($A' = 0.67$, $n = 6$; PPA sites; $P < 0.05$).

Electrophysiological Responses Outside PPHG

Spatial frames of reference manipulation involved several cortical foci outside PPHG (Supporting Information Table S1). Left RSC was recorded in one patient (Fig. 7a). Both egocentric and allocentric conditions induced a gamma-band increase in RSC when compared to control condition. Furthermore, allocentric trials induced higher gamma-band activity compared to egocentric trials between 350 and 650 ms poststimulus onset (Fig. 7b,c; $P < 0.05$). Estimation of signal strength (RSC selectivity to a given frame of reference) based on gamma amplitude levels was higher in allocentric trials (Fig. 7d), although egocentric trials could also be decoded with a classification performance above chance level.

A cluster within the medial fusiform gyrus (MFUG, $n = 10$ sites, Supporting Information Table S1) was very close to PPHG. Given the variability of COS, patients' MRI slices were inspected to dissociate MFUG and PPHG sites based on anatomical landmarks [Pruessner et al., 2002]. Allocentric trials induced stronger gamma activities compared to egocentric and control trials ($P < 0.05$, Supporting Information Fig. S3a) in MFUG sites. The timing of this effect was similar to PPHG sites. For one patient (P8), we could test whether MFUG activities were modulated by visual categories. MFUG gamma-band amplitude was higher for scene stimuli compared to all other categories, suggesting that this MFUG site was also within PPA. Task-related gamma activities were only found in two other brain regions: in the depth of the left middle temporal gyrus (P1 d′5, Supporting Information Fig. S3b), and in the middle occipital gyrus, (MOG; P1, w′11, Supporting Information Table S1). In both sites, allocentric trials induced the highest gamma response ($P < 0.05$, KW tests FDR corrected). Therefore, the selectivity across brain regions of gamma-band amplitude in this study was very high (above 900 electrode contacts were examined). Finally, we found two frontoparietal sites where gamma amplitude was selectively higher during egocentric trials (in the right supramarginal gyrus and in the inferior frontal gyrus, Supporting Information Table S1 and Fig. S4).

Although this article focuses on high-frequency amplitude modulations, lower frequency bands, and ERPs were always examined. Spatial frame of reference manipulation modulated selectively only ERPs. Overall, ERPs data were in agreement with gamma-band activities, although the spatial overlap was far from being ideal (Supporting Information Fig. S5). A specific comparison of evoked and induced

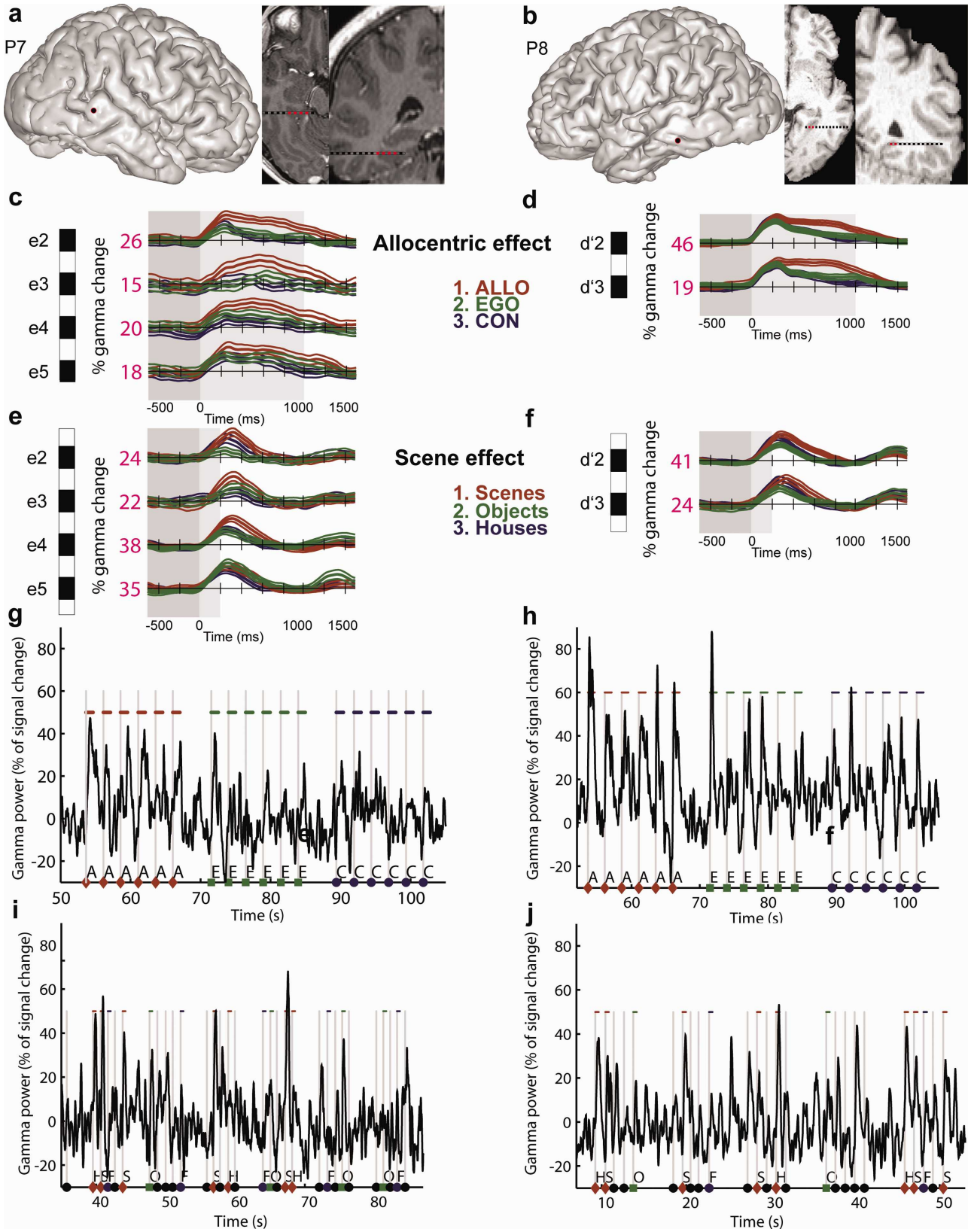
a
P7
b
P8
c
e2
e3
e4
e5
% gamma change
26
15
20
18
-500
0
1000
1500
Time (ms)
Allocentric effect
1. ALLO
2. EGO
3. CON
d
d'2
d'3
46
19
e
24
22
38
35
Scene effect
1. Scenes
2. Objects
3. Houses
f
41
24
g
Gamma power (% of signal change)
Time (s)
h
i
j

Figure 6.

brain response is beyond the scope of this study but can be found in another study by our group [Vidal et al., 2011].

DISCUSSION

PPHG and RSC are involved in spatial orientation [Aguirre et al., 1998; Committeri et al., 2004; Epstein, 2008; Epstein and Kanwisher, 1998; Janzen and van Turennout, 2004; Maguire et al., 1998; Park et al., 2007]. Here, we sought to further examine the functional role of PPHG and RSC with sEEG while patients performed distance judgments made either with reference to the patient's viewpoint (egocentric condition) or with reference to a landmark within the environment (allocentric condition). The main finding of this study was that allocentric trials induced higher gamma (50–150 Hz) amplitude in the PPHG and RSC. Furthermore, electrophysiological activity comprised temporally organized gamma amplitude variations dependent on task constraints, reflecting distinct information processing stages within PPHG.

Gamma-band time course in PPHG/RSC was stereotyped within the first 200 ms in Experiments 1 and 2 (though gamma amplitude was above baseline levels). At latencies inferior to 200 ms, the increase of gamma amplitude could reflect a nonspecific visual response (processing stage 1).

Conversely, between 200 and 500 ms after stimulus onset, gamma-band amplitude became selective to scene stimuli (compared to other visual categories) in PPGH (PPHG processing stage 2). The timing of this second processing stage fits well with the time delays reported for human PPHG neurons decoding visual categories such as famous faces, landmarks, animals, or objects [Mormann et al., 2008]. The robust and reliable scene selectivity found within PPHG in this study contrasts with a previous study using invasive parahippocampal recordings [Kraskov et al., 2007]: both differences in the anatomical locations of the recordings, and in the recording technique (microelectrodes recordings) could account for this discrepancy. Therefore, this study is the first electrophysiological proof regarding the specific involvement of PPHG during scene stimuli processing, compared to other visual categories. The selectivity of gamma-band amplitude to scene stimuli in PPHG is in line with previous neuroimaging findings that identified a PPA [Epstein and Higgins, 2007; Epstein et al., 1999; Epstein and Kanwisher, 1998; Hasson et al., 2003; O'Craven and Kanwisher, 2000; Park et al., 2007]. Interestingly, our results also indicate that PPA responses in the visual localizer experiment are not locked to stimulus duration (200 ms) but extends well beyond stimulus offset, in line with a recent report using other stimulus categories [Quiroga et al., 2008].

A third processing stage was found from 400 to 600 ms poststimulus onset: during this interval, PPHG gamma amplitude was stronger when a spatial evaluation had to be performed (either using an egocentric or an allocentric frame of reference), compared to control trials. Finally, a fourth processing stage was detected from 600 to 800 ms poststimulus onset: during this interval, PPHG gamma amplitude was longer during allocentric than egocentric and control trials. The longer activity observed during allocentric trials is consistent with a recent study that contrasted allocentric and egocentric spatial navigation strategies [Gramann et al., 2011]. The authors, using EEG, found a longer activity in the temporal lobe and the RSC in allocentric navigators. Our results also converge with other data pointing to allocentric-related function implemented in the medial temporal cortex [for a review, see Galati et al., 2010]. This allocentric function would correspond to the automatic activation of an enduring representation of the stable spatial features of the familiar environment [Committeri et al., 2004; Galati et al., 2010; Landgraf et al., 2010]. Here, we showed that such allocentric process triggered higher gamma-band amplitude within PPHG compared to the egocentric condition (in the 600–800 ms range). This gamma amplitude increase cannot be explained by a visual response of PPA to scene stimuli, as identical stimuli were used in all three spatial conditions. PPA activations that are independent from physical stimulus properties were previously reported using several paradigms that examined boundary extension effects [Park et al., 2007] and mental navigation and/or landmark recollection from memory effects [Janzen and van Turennout, 2004; Maguire et al., 1998]. Gamma-band amplitude increases during allocentric trials were so reliable across trials that this activity could be used to predict patients' performance based on the single trial gamma-band amplitude levels: we were able to predict whether the patient was performing an allocentric judgment with a striking accuracy. PPHG/RSC readout was in line with previous

Figure 6.

Gamma-band responses in PPA dissociate two processing stages, across and within trials. (**a** and **b**) Anatomical location of PPA sites. (**c**–**f**) Average (across trials) scene and allocentric effects in individual PPA sites (conventions are similar to Fig. 3). Scenes induced a stronger and longer gamma activity relative to other visual categories. This effect occurred and ended strikingly earlier than the allocentric effect (compare c–e and d–f panels). (**g**–**j**) Raw single trials gamma-band activity recorded in a typical PPA site (P7 e2 and P8, d′2) during the first (g and h) and second (i and j) experiment. The effect of allocentric coding (Allo > Ego) and scene encoding (Scene > Objects) can be directly seen within single trials gamma-band activity. In Experiment 1, the highest peaks and longer gamma increases corresponded to the Allo judgments, whereas in Experiment 2, the highest peaks corresponded to scenes stimuli. A, allocentric; E, egocentric; C, control; S, scene; H, house; F, face; O, objects. [Color figure can be viewed in the online issue, which is available at wileyonlinelibrary.com.]

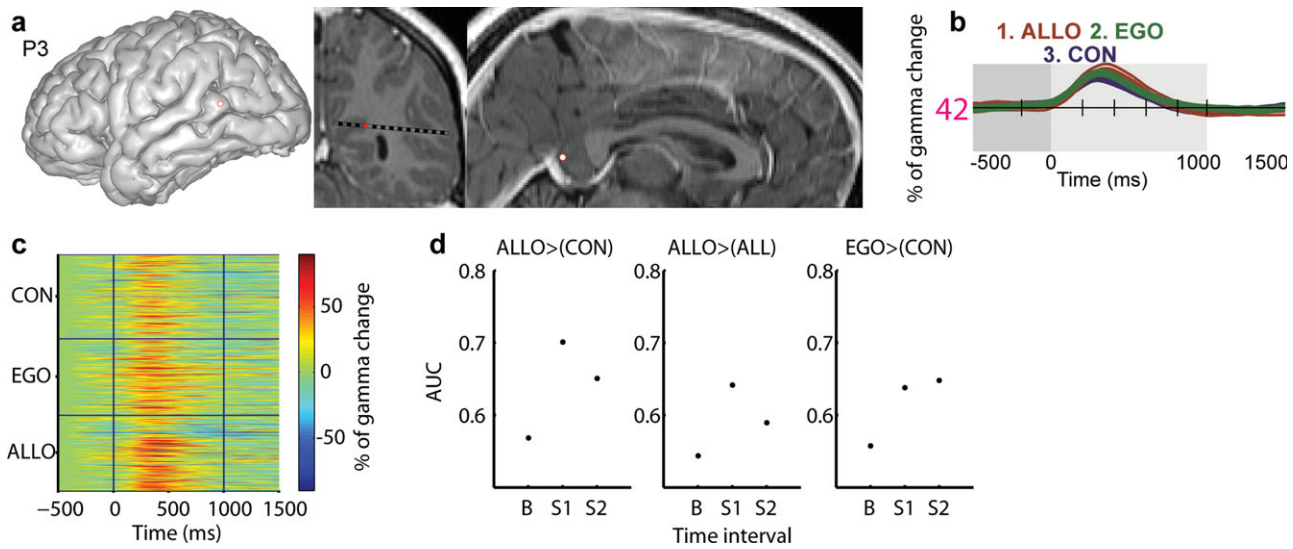

Figure 7.

Retrosplenial cortex gamma-band amplitude was highest in allocentric trials. (**a**) Anatomical location of RSC site (entry point and patient MRI slices). (**b**) Average gamma-band time course as a function of experimental conditions. (**c**) Single trial gamma-band amplitude (in percentage of signal change). (**d**) RSC readout index values (ROC area under curve, AUC). Figure conventions are similar to Figures 3 and 5. [Color figure can be viewed in the online issue, which is available at wileyonlinelibrary.com.]

reports using the same type of procedure to decode information relative to visual categories [Liu et al., 2009; Quiroga et al., 2008; Vidal et al., 2010].

Turning next to RSC, there was a selective increase of gamma-band amplitude during allocentric trials in the 350–650 ms range. This result confirms that RSC is part of the network implementing allocentric frame of reference use in spatial perception [Committeri et al., 2004; Galati et al., 2010]. Both RSC and PPHG lesions impair topographical orientation [Habib and Sirigu, 1987; Maguire, 2001], and both regions play a central role in the identification of specific locations within scenes [Epstein and Higgins, 2007]. In this study, RSC and PPHG were both selectively activated when patients used an environmental landmark to perform the task, in line with a recent study [Morgan et al., 2011]. However, several arguments suggest that RSC and PPHG also play distinct roles, which are not incompatible with the present findings. First, RSC lesion impairs patients' ability to use landmarks to find their way in a familiar environment, despite intact landmark recognition ability [Aguirre and D'Esposito, 1999; Takahashi et al., 1997], whereas PPHG lesions impair patients' ability to learn new paths in novel environments, because of their inability to encode local scenes [Epstein, 2008; Habib and Sirigu, 1987]. Second, RSC is involved in formation and use of cognitive maps [Iaria et al., 2007; Iaria et al., 2009], in the spatial computations based on the environment surrounding the viewed scene [Epstein and Higgins, 2007; Epstein et al., 2007; Park and Chun, 2009], and in the retrieval of familiar scene information [Epstein and Higgins, 2007; Morgan et al., 2011], whereas PPHG is involved in computing spatial layout and relationships within a scene [Epstein, 2008]. In line with these distinctions, a neuroimaging experiment using a task similar to this study [Galati et al., 2010] showed a differential activation of RSC and PPHG: in that experiment, allocentric trials were performed when subjects viewed scenes where the building was not directly visible, so that subjects had to use the environment surrounding the visible scene (to a greater extent compared to this study) to perform the task. The authors found higher activation in RSC in this condition. Here, RSC gamma increase during allocentric trials was briefer and was selective earlier compared to PPHG. Therefore, RSC could trigger the top-down long-latency increase of gamma band in PPHG during allocentric trials. Unfortunately, we could not test this hypothesis because PPHG and RSC were not recorded simultaneously because none of the patients was implanted in both structures.

Despite its strengths, this study has several limitations. Data could reflect the pathological condition of epileptic patients. We suggest that our data primary reflect physiological mechanisms for three reasons. First, trials showing any type of epileptiform activity were discarded. Second, brain regions within epileptogenic networks were not analyzed. Third, similar effects induced by experimental conditions were obtained in patients who had different types of epileptogenic networks and anticonvulsant medication. Another limitation inherent to sEEG is the limited coverage of the brain provided by invasive recordings [Jerbi et al., 2009]. However, the brain networks supporting

control, egocentric, and allocentric trials were known from a previous fMRI study [Committeri et al., 2004]. We showed that several depth electrodes contacts of this study were within these regions of interest, and that gamma-band amplitude modulations were selectively found in these regions.

Altogether, the present findings provide novel evidence regarding the temporal organization of information processing in PPA/PPHG and point to the importance of gamma-band oscillations. A tight coupling between bold signal and gamma-band amplitude modulations was repeatedly demonstrated [Lachaux et al., 2007; Niessing et al., 2005]; Hence, in this study, we predicted that gamma amplitude should increase not only when patients viewed scene but also when patients had to use an allocentric frame of reference. However, the temporal dynamics of these processes was unknown. We found timely separated increases of gamma-band amplitude within PPHG. A first increase of gamma-band amplitude in the PPHG corresponded to a scene selective increase. This is the first functional definition of PPA using direct human brain recordings and is therefore an important confirmation of previous functional neuroimaging reports. A longer latency processing stage within PPHG was identified (i.e., it followed the scene selective increase). This second information processing stage corresponded to allocentric processing and was also found in RSC. These findings suggest that PPHG scene selectivity could correspond to a short-latency bottom-up process whereas allocentric processing within PPHG could correspond to a long latency top-down modulation, possibly triggered by RSC.

ACKNOWLEDGMENTS

The authors thank Patricia Boschetti, Carole Chatelard, and Véronique Dorlin for their invaluable technical help and Véronique Coizet and Olivier David for their precious comments on the manuscript.

REFERENCES

Aguirre GK, D'Esposito M (1999): Topographical disorientation: A synthesis and taxonomy. Brain 122(Pt 9):1613–1628.

Aguirre GK, Zarahn E, D'Esposito M (1998): An area within human ventral cortex sensitive to "building" stimuli: Evidence and implications. Neuron 21:373–383.

Bar M (2004): Visual objects in context. Nat Rev Neurosci 5:617–629.

Boccara CN, Sargolini F, Thoresen VH, Solstad T, Witter MP, Moser EI, Moser MB (2010): Grid cells in pre- and parasubiculum. Nat Neurosci 13:987–994.

Bohbot VD, Kalina M, Stepankova K, Spackova N, Petrides M, Nadel L (1998): Spatial memory deficits in patients with lesions to the right hippocampus and to the right parahippocampal cortex. Neuropsychologia 36:1217–1238.

Britten KH, Shadlen MN, Newsome WT, Movshon JA (1992): The analysis of visual motion: A comparison of neuronal and psychophysical performance. J Neurosci 12:4745–4765.

Burgess N (2006): Spatial memory: How egocentric and allocentric combine. Trends Cogn Sci 10:551–557.

Burgess N, O'Keefe J (2011): Models of place and grid cell firing and theta rhythmicity. Curr Opin Neurobiol 21:1–11.

Caplan JB, Madsen JR, Schulze-Bonhage A, Aschenbrenner-Scheibe R, Newman EL, Kahana MJ (2003): Human theta oscillations related to sensorimotor integration and spatial learning. J Neurosci 23:4726–4736.

Chen LL, Lin LH, Green EJ, Barnes CA, McNaughton BL (1994): Head-direction cells in the rat posterior cortex. I. Anatomical distribution and behavioral modulation. Exp Brain Res 101:8–23.

Committeri G, Galati G, Paradis AL, Pizzamiglio L, Berthoz A, LeBihan D (2004): Reference frames for spatial cognition: Different brain areas are involved in viewer-, object-, and landmark-centered judgments about object location. J Cogn Neurosci 16:1517–1535.

Ekstrom AD, Kahana MJ, Caplan JB, Fields TA, Isham EA, Newman EL, Fried I (2003): Cellular networks underlying human spatial navigation. Nature 425:184–188.

Epstein R, Harris A, Stanley D, Kanwisher N (1999): The parahippocampal place area: Recognition, navigation, or encoding? Neuron 23:115–125.

Epstein R, Kanwisher N (1998): A cortical representation of the local visual environment. Nature 392:598–601.

Epstein RA (2008): Parahippocampal and retrosplenial contributions to human spatial navigation. Trends Cogn Sci 12:388–396.

Epstein RA, Higgins JS (2007): Differential parahippocampal and retrosplenial involvement in three types of visual scene recognition. Cereb Cortex 17:1680–1693.

Epstein RA, Parker WE, Feiler AM (2007): Where am I now? Distinct roles for parahippocampal and retrosplenial cortices in place recognition. J Neurosci 27:6141–6149.

Epstein RA, Ward EJ (2009): How reliable are visual context effects in the parahippocampal place area? Cereb Cortex 20:294–303.

Furtak SC, Wei SM, Agster KL, Burwell RD (2007): Functional neuroanatomy of the parahippocampal region in the rat: The perirhinal and postrhinal cortices. Hippocampus 17:709–722.

Galati G, Pelle G, Berthoz A, Committeri G (2010): Multiple reference frames used by the human brain for spatial perception and memory. Exp Brain Res 206:109–120.

Genovese CR, Lazar NA, Nichols T (2002): Thresholding of statistical maps in functional neuroimaging using the false discovery rate. Neuroimage 15:870–878.

Gramann K, Onton J, Riccobon D, Mueller HJ, Bardins S, Makeig S (2011): Human brain dynamics accompanying use of egocentric and allocentric reference frames during navigation. J Cogn Neurosci 22:2836–2849.

Habib M, Sirigu A (1987): Pure topographical disorientation: A definition and anatomical basis. Cortex 23:73–85.

Hasson U, Harel M, Levy I, Malach R (2003): Large-scale mirror-symmetry organization of human occipito-temporal object areas. Neuron 37:1027–1041.

Iaria G, Bogod N, Fox CJ, Barton JJ (2009): Developmental topographical disorientation: Case one. Neuropsychologia 47:30–40.

Iaria G, Chen JK, Guariglia C, Ptito A, Petrides M (2007): Retrosplenial and hippocampal brain regions in human navigation: Complementary functional contributions to the formation and use of cognitive maps. Eur J Neurosci 25:890–899.

Jacobs J, Kahana MJ, Ekstrom AD, Mollison MV, Fried I (2010): A sense of direction in human entorhinal cortex. Proc Natl Acad Sci USA 107:6487–6492.

Janzen G, van Turennout M (2004): Selective neural representation of objects relevant for navigation. Nat Neurosci 7:673–677.

Jerbi K, Ossandon T, Hamame CM, Senova S, Dalal SS, Jung J, Minotti L, Bertrand O, Berthoz A, Kahane P, Lachaux JP (2009): Task-related gamma-band dynamics from an intracerebral perspective: review and implications for surface EEG and MEG. Hum Brain Mapp 30:1758–1771.

Kraskov A, Quiroga RQ, Reddy L, Fried I, Koch C (2007): Local field potentials and spikes in the human medial temporal lobe are selective to image category. J Cogn Neurosci 19:479–492.

Lachaux JP, Fonlupt P, Kahane P, Minotti L, Hoffmann D, Bertrand O, Baciu M (2007): Relationship between task-related gamma oscillations and BOLD signal: New insights from combined fMRI and intracranial EEG. Hum Brain Mapp 28:1368–1375.

Lachaux JP, Rudrauf D, Kahane P (2003): Intracranial EEG and human brain mapping. J Physiol Paris 97:613–628.

Landgraf S, Krebs MO, Olie JP, Committeri G, van der Meer E, Berthoz A, Amado I (2010): Real world referencing and schizophrenia: Are we experiencing the same reality? Neuropsychologia 48:2922–2930.

Lever C, Burton S, Jeewajee A, O'Keefe J, Burgess N (2009): Boundary vector cells in the subiculum of the hippocampal formation. J Neurosci 29:9771–9777.

Liu H, Agam Y, Madsen JR, Kreiman G (2009): Timing, timing, timing: Fast decoding of object information from intracranial field potentials in human visual cortex. Neuron 62:281–290.

Maguire EA (2001): The retrosplenial contribution to human navigation: A review of lesion and neuroimaging findings. Scand J Psychol 42:225–238.

Maguire EA, Burgess N, Donnett JG, Frackowiak RS, Frith CD, O'Keefe J (1998): Knowing where and getting there: A human navigation network. Science 280:921–924.

Morgan LK, Macevoy SP, Aguirre GK, Epstein RA (2011): Distances between real-world locations are represented in the human hippocampus. J Neurosci 31:1238–1245.

Mormann F, Kornblith S, Quiroga RQ, Kraskov A, Cerf M, Fried I, Koch C (2008): Latency and selectivity of single neurons indicate hierarchical processing in the human medial temporal lobe. J Neurosci 28:8865–8872.

Moser EI, Kropff E, Moser MB (2008): Place cells, grid cells, and the brain's spatial representation system. Annu Rev Neurosci 31:69–89.

Niessing J, Ebisch B, Schmidt KE, Niessing M, Singer W, Galuske RA (2005): Hemodynamic signals correlate tightly with synchronized gamma oscillations. Science 309:948–951.

O'Craven KM, Kanwisher N (2000): Mental imagery of faces and places activates corresponding stiimulus-specific brain regions. J Cogn Neurosci 12:1013–1023.

O'Keefe J (1976): Place units in the hippocampus of the freely moving rat. Exp Neurol 51:78–109.

Park S, Chun MM (2009): Different roles of the parahippocampal place area (PPA) and retrosplenial cortex (RSC) in panoramic scene perception. Neuroimage 47:1747–1756.

Park S, Intraub H, Yi DJ, Widders D, Chun MM (2007): Beyond the edges of a view: Boundary extension in human scene-selective visual cortex. Neuron 54:335–342.

Pruessner JC, Kohler S, Crane J, Pruessner M, Lord C, Byrne A, Kabani N, Collins DL, Evans AC (2002): Volumetry of temporopolar, perirhinal, entorhinal and parahippocampal cortex from high-resolution MR images: Considering the variability of the collateral sulcus. Cereb Cortex 12:1342–1353.

Quiroga RQ, Mukamel R, Isham EA, Malach R, Fried I (2008): Human single-neuron responses at the threshold of conscious recognition. Proc Natl Acad Sci USA 105:3599–3604.

Sugar J, Witter MP, van Strien NM, Cappaert NL (2011): The retrosplenial cortex: Intrinsic connectivity and connections with the (para)hippocampal region in the rat. An interactive connectome. Front Neuroinform 5:7.

Takahashi N, Kawamura M, Shiota J, Kasahata N, Hirayama K (1997): Pure topographic disorientation due to right retrosplenial lesion. Neurology 49:464–469.

Taube JS (2007): The head direction signal: Origins and sensory-motor integration. Annu Rev Neurosci 30:181–207.

Taube JS, Muller RU, Ranck JB Jr (1990): Head-direction cells recorded from the postsubiculum in freely moving rats. I. Description and quantitative analysis. J Neurosci 10:420–435.

Vidal JR, Ossandon T, Jerbi K, Dalal SS, Minotti L, Ryvlin P, Kahane P, Lachaux JP (2010): Category-specific visual responses: An Intracranial Study comparing gamma, beta, alpha, and ERP response selectivity. Front Hum Neurosci 4:195.

Vidal JR, Ossandon T, Jerbi K, Dalal SS, Minotti L, Ryvlin P, Kahane P, Lachaux JP (2011): Category-specific visual Responses: An Intracranial Study comparing gamma, beta, alpha, and ERP response selectivity. Front Hum Neurosci 4:195.